

Preconcentration, Separation, and Indirect Detection of Nonfluorescent Analytes Using Fluorescent Mobility Markers

Tarun K. Khurana and Juan G. Santiago*

Department of Mechanical Engineering, Stanford University, Stanford, California 94305

We present a method to achieve separation and indirect detection of nonfluorescent species using fluorescent mobility markers. This technique leverages isotachophoresis (ITP) for both preconcentration and separation. We employ a leading electrolyte (LE), trailing electrolyte (TE), and a set of fluorescent markers of mobilities designed to bound those of nonfluorescent analytes of interest. Fluorescent markers and nonfluorescent analytes are initially mixed homogeneously and ITP is initiated. The dynamics of isotachophoresis cause the analyte and fluorescent marker mixture to segregate into respective zones between the LE and TE in the order of reducing mobility. Unlabeled analytes are detected as gaps (regions with local minimums in intensity) in the fluorescent signals of mobility markers. We have successfully demonstrated preconcentration, separation, and detection of unlabeled amino acids serine, glycine, and phenylalanine; and of acetic acid, aspartic acid, and 3-phenylpropionic acid. We show detection of 12 μM concentration of analytes with signal-to-noise ratio of 4.0 and with a high degree of repeatability. We discuss methods for encoding mobility marker identity using marker fluorescence intensity level and alternating fluorescence emission wavelengths. We present example experimental results of fluorescence intensity level encoding.

Since the inception of micro total analysis systems,¹ fluorescence detection has remained the most popular method of detection for microfluidic platforms due to its high sensitivity and ease of application in microfabricated devices.^{2–4} Fluorescent labeling has been used for on-chip analyses of amino acids;⁵ DNA fragments, and proteins (reviewed by Dolnik et al.⁶), and amino sugars⁷ among others. A major constraint of fluorescence detection

is that the analyte should possess either native fluorescence or, for example, have a free amine, thiol, or hydroxyl group that can be derivatized. Other detection schemes such as UV absorbance^{8,9} and electrochemical detection^{10,11} have been used, but these typically offer less sensitivity^{12,13} and are more difficult to implement on chip (discussed later in this section).

Traditional indirect detection methods using either fluorescence or UV absorbance offer alternate solutions to fluorescent labeling.^{14–16} These methods employ strongly UV-absorbing/fluorescent markers, which are added to the entire background buffer to yield a uniform background signal. Nonfluorescent/non-UV-absorbing analyte species are then injected into a separation channel and separated via capillary zone electrophoresis. As analytes separate and disperse, they locally displace the background marker as per the requirements of electroneutrality and current conservation.¹⁷ The local reduction in the signal of marker ions provides an indirect detection of the analyte zone. These traditional indirect detection methods offer no preconcentration and are usually limited to analyte concentrations above ~ 0.1 mM.¹³ The technique is also susceptible to false positive identifications due to the presence of system peaks¹⁸ and fluctuations in background signal due to Joule heating and unsteady illumination.^{19,20} A detailed review of indirect detection in capillaries was presented by Johns et al.²¹ Indirect fluorescence detection has also been used in microchips,^{22,23} but with similar drawbacks.²⁴

* To whom correspondence should be addressed. E-mail: juan.santiago@stanford.edu. Fax: (650) 723-7657.

- (1) Manz, A.; Graber, N.; Widmer, H. M. *Sens. Actuators, B1* **1990**, *1*, 244–248.
- (2) Harrison, D. J.; Fan, Z. H.; Seiler, K.; Manz, A.; Widmer, H. M. *Anal. Chim. Acta* **1993**, *283*, 361–366.
- (3) Jacobson, S. C.; Hergenroder, R.; Moore, A. W.; Ramsey, J. M. *Anal. Chem.* **1994**, *66*, 4127–4132.
- (4) Fister, J. C.; Jacobson, S. C.; Ramsey, J. M. *Anal. Chem.* **1999**, *71*, 4460–4464.
- (5) Skelley, A. M.; Mathies, R. A. *J. Chromatogr., A* **2003**, *1021*, 191–199.
- (6) Dolnik, V.; Liu, S.; Jovanovich, S. *Electrophoresis* **2000**, *21*, 41–54.
- (7) Suzuki, S.; Shimotsu, N.; Honda, S.; Arai, A.; Nakanishi, H. *Electrophoresis* **2001**, *22*, 4023–4031.

- (8) Guihen, E.; Glennon, J. D. *J. Chromatogr., A* **2005**, *1071*, 223–228.
- (9) Ludwig, M.; Kohler, F.; Belder, D. *Electrophoresis* **2003**, *24*, 3233–3238.
- (10) Woolley, A. T.; Lao, K.; Glazer, A. N.; Mathies, R. A. *Anal. Chem.* **1998**, *70*, 684–688.
- (11) Prest, J. E.; Baldock, S. J.; Fielden, P. R.; Brown, B. J. *Analyst* **2001**, *126*, 433–437.
- (12) Götz, S.; Karst, U. *Anal. Bioanal. Chem.* **2007**, *387*, 183–192.
- (13) Landers, J. P. *Handbook of Capillary Electrophoresis*; CRC Press: Boca Raton, FL, 1994.
- (14) Hjertén, S. S.; Elenbring, K. K.; Kilár, F. F.; Liao, J. L.; Chen, A. J.; Siebert, C. J.; Zhu, M. D. *J. Chromatogr., A* **1987**, *403*, 47–61.
- (15) Foret, F.; Fanali, S.; Ossicini, L.; Bocek, P. *J. Chromatogr., A* **1989**, *470*, 299–308.
- (16) Kuhr, W. G.; Yeung, E. S. *Anal. Chem.* **1988**, *60*, 2642–2646.
- (17) Poppe, H. *J. Chromatogr., A* **1990**, *506*, 45–60.
- (18) Gas, B.; Kenndler, E. *Electrophoresis* **2004**, *25*, 3901–3912.
- (19) Bruin, G. J. M. *J. Chromatogr., A* **1992**, *608*, 97–107.
- (20) Xu, X.; Kok, W. T.; Poppe, H. *J. Chromatogr., A* **1997**, *786*, 333–345.
- (21) Johns, C.; Macka, M.; Haddad, P. R. *Electrophoresis* **2003**, *24*, 2150–2167.
- (22) Munro, N. J.; Huang, Z. L.; Finegold, D. N.; Landers, J. P. *Anal. Chem.* **2000**, *72*, 2765–2773.
- (23) Arundell, M.; Whalley, P. D.; Manz, A. *Fresenius' J. Anal. Chem.* **2000**, *367*, 686–691.
- (24) Schwarz, M. A.; Hauser, P. C. *Lab Chip* **2001**, *1*, 1–6.

We present here an indirect detection technique that is based on isotachopheresis (ITP) with fluorescent mobility markers. Isotachopheresis has remained a popular preconcentration and separation technique for over three decades.^{25–30} The technique uses an imposed electrophoretic mobility gradient to create concentrated analyte zones with nondispersing interfaces. Sample ions to be stacked and separated are typically introduced between a leading (LE) and trailing electrolyte (TE) with mobilities respectively higher and lower than those of sample species. Under the influence of an electric field, sample ions redistribute themselves in sequential zones in order of reducing mobility (starting from LE to TE). After initial transients, ITP-based separations typically result in adjacent, contiguous zones of analytes moving at identical speeds. These ITP zones have been traditionally detected using UV absorbance and conductivity detection techniques on a capillary platform.³¹ For on-chip devices, UV absorbance detection typically results in poor detection sensitivity due to short optical path length.¹² Conductivity detection requires microfabrication of integrated electrodes to obtain reasonable detection sensitivity (~0.1 mM). The conductivity detection signals are a strong function of electrode design geometry, require external circuits for isolating separation and detection voltages, and are a strongly impacted by electrode surface condition and fouling.^{32,33}

A few ITP studies have employed nondetectable spacer ions to improve resolution of the detectable analyte zones. Spacer ions with mobilities intermediate to those of directly detectable analytes are added to the sample mixture. At steady state, this traditional use of spacers results in undetectable spacer zones segregating detectable analyte species and thereby increasing analyte resolution. The technique has been used exclusively for UV-absorbent/detectable analytes with non-UV-absorbent/undetectable spacers.^{34–36}

We here propose a new indirect detection technique that leverages ITP and directly detectable fluorescent markers to concentrate, separate, and indirectly detect and quantify the concentration of unlabeled (nonfluorescent) analytes. We use directly detectable fluorescent markers to detect directly undetectable analytes. ITP is used to focus and separate initially mixed markers and analytes into their respective zones in order of reducing mobility. The fluorescent markers segregate nonfluorescent analyte zones and yield quantitative mobility and concentration information of analytes. The presence of unlabeled analytes

is detected as local minimums or “gaps” in the signal of the fluorescent markers. The (known) mobilities of the two fluorescent markers that bracket each analyte zone provide an upper and lower bound for the analyte’s mobility; so analyte mobility is resolved within the resolution offered by the marker “ladder”. The initial concentration of unlabeled analytes is a linear function of the spacing between the adjacent fluorescent markers. Our technique simultaneously preconcentrates and separates analytes via ITP and is not susceptible to the ambiguities of system peaks. The technique requires no labeling of analytes and minimizes sample preparation, while leveraging the sensitivity, convenience, and ubiquity of fluorescence detectors.

We demonstrate and quantify the performance of the ITP fluorescent marker assay to separate and detect the unlabeled amino acids serine and phenylalanine (and glycine) using three fluorescent marker species (Oregon Green carboxylic acid, fluorescein, and Bodipy). Using these commercially available fluorescent markers, we show separation and detection of acetic acid, aspartic acid, and 3-phenylpropionic acid, with a limit of detection of ~12 μM. We also demonstrate encoding strategies that unambiguously identify these fluorescent mobility markers and that can be extended to an arbitrary number of mobility markers.

THEORY

We first discuss a simple anionic ITP case where all analytes are fully ionized and present in sufficiently high initial concentration to form analyte zones with a plateau (locally uniform) concentration profile at steady state. The analysis assumes all anionic species (both markers and analytes) in this example have a common counterion.

For the leading ion (L), trailing ion (T), *i*th sample ion (*X_i*), and counterion (A), the Kohlrausch regulating function (KRF) and electroneutrality condition can be used to specify the concentration of *i*th sample ion as,^{29,37}

$$C_{X_i} = C_L \left(\frac{v_{X_i}}{v_L} \right) \left(\frac{v_L + v_A}{v_{X_i} + v_A} \right) \quad (1)$$

Under steady KRF conditions, the length of each analyte zone, *L_{X_i}*, and the length of the injected plug length *L₀* are related as,

$$L_{X_i} = C_{0,X_i} L_0 / C_{X_i} \quad (2)$$

Here *C_{0,X_i}* is the initial concentration of analyte *X_i* and *C_{X_i}* is the final concentration given by eq 1. For an injected analyte mixture of length *L₀*, the steady-state length of an analyte zone *X_i* is then expressed as,

$$L_{X_i} = \left(\frac{v_L}{v_{X_i}} \right) \left(\frac{v_{X_i} + v_A}{v_L + v_A} \right) \frac{C_{0,X_i} L_0}{C_L} \quad (3)$$

We note that this length estimate assumes that the ITP zone width is significantly larger than the thickness of the interface between zones.³⁸ For low initial concentrations (and short times), the ITP

(25) Everaerts, F. M.; Beckers, J. L.; Verheggen, T. P. E. M. *Isotachopheresis: Theory, Instrumentation, and Applications*; Elsevier Scientific Publishing: New York, 1976.

(26) Bodor, R.; Madajova, V.; Kaniansky, D.; Masar, M.; Johnck, M.; Stanislawski, B. *J. Chromatogr., A* **2001**, *916*, 155–165.

(27) Dolnik, V.; Deml, M.; Bocék, P. *J. Chromatogr., A* **1985**, *320*, 89–97.

(28) Hirokawa, T.; Ohmori, A.; Kiso, Y. *J. Chromatogr., A* **1993**, *634*, 101–106.

(29) Jung, B.; Bharadwaj, R.; Santiago, J. G. *Anal. Chem.* **2006**, *78*, 2319–2327.

(30) Wainright, A.; Williams, S. J.; Ciambone, G.; Xue, Q. F.; Wei, J.; Harris, D. *J. Chromatogr., A* **2002**, *979*, 69–80.

(31) Bocek, P.; Deml, M.; Gebauer, P.; Dolnik, V. *Analytical Isotachopheresis*; VCH: New York, 1988.

(32) Chen, L.; Prest, J. E.; Fielden, P. R.; Goddard, N. J.; Manz, A.; Day, P. J. R. *Lab Chip* **2006**, *6*, 474–487.

(33) Macka, M.; Haddad, P. R. *Electrophoresis* **2004**, *25*, 4032–4057.

(34) Oerlemans, F.; Debruyne, C.; Mikkers, F.; Verheggen, T.; Everaerts, F. M. *J. Chromatogr., B* **1981**, *225*, 369–379.

(35) Nagyova, I.; Kaniansky, D. *J. Chromatogr., A* **2001**, *916*, 191–200.

(36) Husmann-Holloway, S.; Borriess, E. *Fresenius’ J. Anal. Chem.* **1982**, *311*, 465–466.

(37) Martin, A. J. P.; Everaerts, F. M. *Proc. R. Soc. London, Ser. A* **1970**, *316*, 493–514.

zone width can be on the order of the interface width. In that case, analyte peak width (and signal intensity) is a function of both initial concentration and injected length.^{29,39} This regime of ITP has been called the spike mode,³⁵ where concentration profile of analyte zone is approximately Gaussian rather than plateau shaped. We here show ITP separations of nonfluorescent analytes with $\sim 10 \mu\text{M}$ concentrations and higher (for 5 mM LE), and so analyte zones form well-defined plateau zones at steady state. In contrast, we use relatively low fluorescent marker concentrations ($\sim 50 \text{ nM}$), and so these mobility markers are in the spike mode. Having these markers in spike mode allows us to encode their identity by varying their post-ITP signal strength in a set pattern.

In general, when the species are weak electrolytes (e.g., weak acids/bases), the effective species mobility depends on local ionic strength, dissociation constant, and local pH, all of which contribute to the degree of ionization. The pH of each ITP (analyte or marker) zone is controlled largely by pH of the LE zone.⁴⁰ A comprehensive treatment of ITP dynamics requires solution of the species conservation equations coupled with treatment of acid–base equilibrium reactions⁴¹ and ionic interactions. The most recent electrophoresis simulation codes (Simul and Peakmaster) developed by Gas et al.⁴² include the effect of pH and ionic interactions. A freeware version of Peakmaster and Simul is available on the Web.⁴³ For the current work, we chose to demonstrate our assay in a regime where analytes are fully ionized and we used Simul to model most of our experiments.

EXPERIMENTAL SECTION

Materials and Instrumentation. The analyte concentration sensitivity range of the current assay can be “tuned” by varying the concentration of LE. To demonstrate this, we performed experiments using relatively high and low LE concentrations corresponding to low- and high-sensitivity analyte detection. We first describe the high LE concentration ITP-marker experiments, where we used 350 mM Tris-HCl (titrated to pH 10.2 with sodium hydroxide) as the LE and 50 mM sodium tetraphenylborate as the TE. For these cases, we prepared 50 mM stock solutions of Tris–serine and Tris–phenylalanine as sample analytes. These amino acids have respective pK_a values of 9.3 and 9.26. The amino acids, LE, and TE reagents were obtained from Sigma Aldrich (St. Louis, MO). The fluorescent markers were Oregon Green carboxylic acid (OGCA), fluorescein, fluorescein isothiocyanate (FITC), and Bodipy and were obtained from Molecular Probes (Eugene, OR). We prepared $10 \mu\text{M}$ concentration stock solutions of these fluorescent markers and diluted their final concentration to 50 nM in the analyte–fluorescent marker mixture. All solutions were prepared using ultrafiltered deionized water (DIUF) from Fischer Scientific (Fair Lawn, NJ). The experiments were performed on commercially available borosilicate microchips with “simple cross” geometry (Micalyne, Alberta, Canada) with wet-etched, $50\text{-}\mu\text{m}$ -wide, and $20\text{-}\mu\text{m}$ -deep channels.

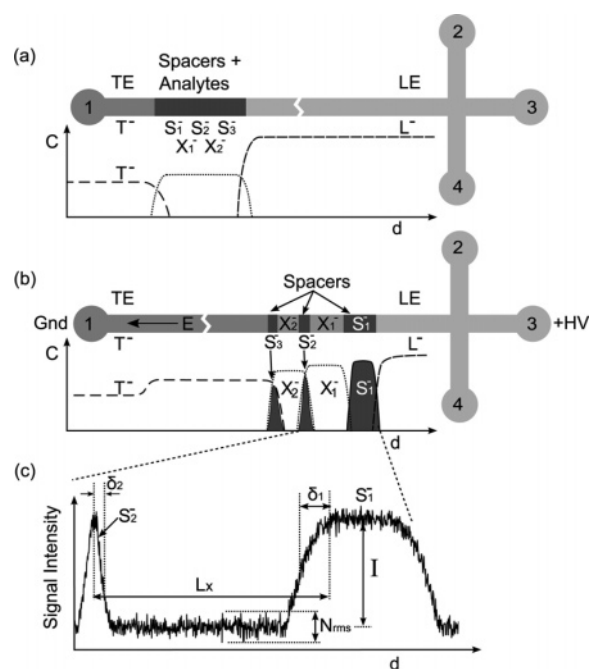


Figure 1. Schematic of ITP-marker experiment protocol. A finite injection volume consisting of the analyte–marker mixture is loaded into the chip between the leading and trailing electrolyte. (a) Under an applied electric field, the analytes (X_i^-) and fluorescent markers (S_i^-) separate into their respective isotachopheric zones between the LE and TE. (b) Given sufficient initial concentration, analyte zones (X_i^-) attain plateau-shaped peaks at steady state. Markers with low initial concentration (S_2^- and S_3^- in this example) do not reach the KRF condition and appear as peaks within the diffused boundary at the interface of adjoining analytes. Parameters associated with figures of merit associated with the assay are shown in schematic c.

For the low LE concentration experiments, the LE and TE were respectively 5 mM Tris-HCl (pH 9.2) and 5 mM sodium tetraphenylborate. The analyte stock solutions were 5 mM sodium salts of acetic acid, aspartic acid, and 3-phenylpropionic acid. The initial concentration of fluorescent markers was 50 nM. We used NS-95 microchip (Caliper, Mountain View, CA) with a simple cross pattern and $34\text{-}\mu\text{m}$ -wide and $12\text{-}\mu\text{m}$ -deep channels. We here applied a positive hydrostatic head to the cathode to counter the electroosmotic flow (EOF) using a P-854X Luer male interconnect (Upchurch Scientific, Oak Harbor, WA). This fluidic port was connected with 1.8-mm-i.d. Tygon tubing to a reservoir with an adjustable height ranging from 0 to 20 cm.

We obtained images using an inverted epifluorescent microscope (IX70, Olympus, Hauppauge, NY) equipped with a mercury lamp, U-MWIBA filtercube from Olympus (460–490 nm excitation, 515 nm emission, and 505 nm cutoff dichroic) and a $10\times$ (NA = 0.4) UPlanApo objective. Images were captured using a 12-bit, 1300×1030 pixel array CCD camera (fx16; Coolsnap, Roper Scientific, Trenton NJ). We controlled the frame grabber using V++ software and processed the images with MATLAB. High voltage was applied in the microchip wells using a computer-controlled Labsmith HVS-3000D (Livermore, CA) power supply.

Assay Protocol. The general assay protocol is depicted schematically in Figure 1. The chip was first filled with LE. Well 1 was then emptied, rinsed 2–3 times (by filling with deionized water and emptying), and filled with the analyte–fluorescent marker mixture. A finite plug, this mixture was injected using

(38) Gebauer, P.; Bocek, P. *Electrophoresis* **1995**, *16*, 1999–2007.

(39) Svoboda, M.; Vacik, J. *J. Chromatogr., A* **1976**, *119*, 539–547.

(40) Everaerts, F. M.; Routs, R. J. *J. Chromatogr., A* **1971**, *58*, 181–194.

(41) Bier, M.; Palusinski, O. A.; Mosher, R. A.; Saville, D. A. *Science* **1983**, *219*, 1281–1287.

(42) Jaros, M.; Vcelakova, K.; Zusková, I.; Gas, B. *Electrophoresis* **2002**, *23*, 2667–2677.

(43) <http://www.natur.cuni.cz/gas/>.

pressure-driven flow by applying a vacuum on well 4 for ~ 10 s (we used an inverted pipet tip with an O-ring at the end to form an imperfect seal between the vacuum line and the chip). We achieved injection lengths of 6 ± 0.2 mm by real-time monitoring of the injection front with the CCD camera. Well 1 was then emptied and filled with the TE. High voltage (~ 1200 V) was then applied from wells 3 to 1 as shown in Figure 1, to initiate ITP.

At high LE concentrations, the axial average EOF velocity was lower in magnitude than the isotachophoretic velocity, and hence, anions migrated toward the anode. For the low LE concentration experiments, EOF dominated over electrophoresis, and in the absence of an external pressure difference, analytes migrated toward the cathode. We therefore used an adjustable-height reservoir connected to well 1 to apply an external pressure difference of ~ 1.5 kPa to counter EOF in low LE experiments. We also here reduced the separation voltage to 600 V.

Signal-to-Noise Ratio (SNR) and Resolution. We here discuss key parameters that quantify the separation efficiency of our ITP-mobility marker assay. Referring to Figure 1c, the SNR for the fluorescent markers, SNR_{fm} can be defined as

$$\text{SNR}_{\text{fm}} = (I/N_{\text{rms}}) \quad (4)$$

where N_{rms} is the standard deviation of the background signal fluctuation and I is the fluorescence intensity signal of the marker. This parameter should be, say, greater than 3 to enable identification of a fluorescent marker. The SNR associated with analyte detection, SNR_{an} , is quite different. Both the presence of an analyte and its initial concentration are inferred from the length of the analyte zone. The analyte zone should therefore be larger than the peak width of the adjacent markers. We here define SNR_{an} for an analyte X_i as follows:

$$\text{SNR}_{\text{an},X_i} = \frac{L_{X_i}}{(\delta_1 + \delta_2)/2} = \frac{L_0}{(\delta_1 + \delta_2)/2} \left(\frac{v_L}{v_{X_i}} \right) \left(\frac{v_{X_i} + v_A}{v_L + v_A} \right) \frac{C_{0,X_i}}{C_L} \quad (5)$$

where δ_1 and δ_2 are the widths of fluorescent marker interfaces adjacent to the analyte and L_{X_i} is the width of the analyte zone (defined here as the distance between the two inflection points associated with δ_1 and δ_2). The equation shows the relation of SNR_{an} to the initial sample plug length L_0 , initial analyte concentration C_{0,X_i} , and LE concentration C_L , assuming KRF condition is achieved for analyte X_i . We recommend SNR_{an} greater than ~ 2 for analyte detection and greater than 3 for accurate estimation of analyte concentration. In the current technique, fluorescent markers typically appear as peaks separating two analyte zones, and their peak width is governed by dispersion and electric field gradient between these adjacent analyte zones.⁴⁴ For a given system, electric field gradient depends on the applied voltage and the mobilities of adjacent analytes.⁴⁵

Last, the mobility of an analyte zone is bounded by the mobility of its adjacent markers. We can describe the resolution on absolute mobility of analyte X_i in terms of mobilities of bounding markers $v_{\text{fm},i}$ and $v_{\text{fm},i+1}$ as

$$R_{X_i} = \frac{v_{\text{fm},i} - v_{\text{fm},i+1}}{(v_{\text{fm},i} + v_{\text{fm},i+1})/2} \quad (6)$$

Therefore, the resolving power of our assay is governed by the mobilities of the fluorescent markers.

In the absence of an intermediate mobility marker, the assay will interpret two or more analytes bounded by the same pair of markers as a single species. However, note that such ambiguity occurs in all displacement electrophoresis techniques (including ITP) and most elution techniques. For example, two analyte zones with closely spaced mobilities would result in very close relative step height values and would appear as a single zone to the conductivity detector. In addition, electrophoretic or chromatographic separations of analytes with closely spaced mobilities yield a single peak in the signal—and this is perforce interpreted as single species. Unlike traditional techniques, however, the current assay offers a unique way of increasing resolution: Incorporation of additional markers in the mobility range of interest. Given its high peak capacity (e.g., we fit four markers and three analytes in less than 2% of 4-cm separation channel length), the resolution is currently limited only by the availability of fluorescent marker species.

RESULTS AND DISCUSSION

Initial Demonstration Assay Using Two Amino Acids (High LE Concentration Case). We first present the high LE concentration ITP-marker experiments for preconcentrating, separating, and detecting two unlabeled amino acids phenylalanine and serine with ~ 10 mM initial concentration. We here adjusted the pH of the LE (350 mM Tris-HCl) to 10.2 by titrating with 5 M NaOH (yielding ~ 325 mM Tris-HCl). This strongly alkaline LE was used to ensure full dissociation of the amino acids in their respective ITP zones.

Measurements quantifying the temporal evolution of the marker and analyte bands are shown in Figure 2. The plots are width-averaged fluorescence intensity versus time and distance along the separation channel. The gray scale is inverted so dark regions correspond to high-intensity fluorescence. The fluorescent markers are initially visible as a single fluorescent peak ($x < 10$ mm, where x is the distance from the TE well) and then evolve into three distinct bands. Note the transitions in the speed/trace slope and the rates of spread of peaks near $x = 10.5$ and 21.5 mm (there is another transition near $x = 14$ mm, not shown). These transitions are not predicted by simple ITP theory. We hypothesize they are associated with the temporal evolution of local pH in the ITP zones. The initial analyte mixture pH is ~ 8.6 , and the amino acids are not fully ionized. As ITP conditions are established, the pH of each ITP zone behind the LE increases due to the influx of Na^+ and Tris^+ ions, and this initiates a process by which the analytes overspeed the TE and markers. The plots serve to demonstrate the rich physics of the transients in ITP process and the SNR of the final signal. This is also to our knowledge the first time such spatiotemporal data are shown for ITP assays. Figure 2d shows the spatiotemporal plot of the steady-state ITP zones where we label the LE, TE, markers, and analytes.

For the rest of our analysis, we shall focus on the $x > 25$ mm region, where the ITP bands acquire steady-state velocity and spacing. We performed an extensive series of calibration and

(44) Saville, D. A. *Electrophoresis* **1990**, *11*, 899–902.

(45) Saville, D. A.; Paluszinski, O. A. *AICHE J.* **1986**, *32*, 207–214.

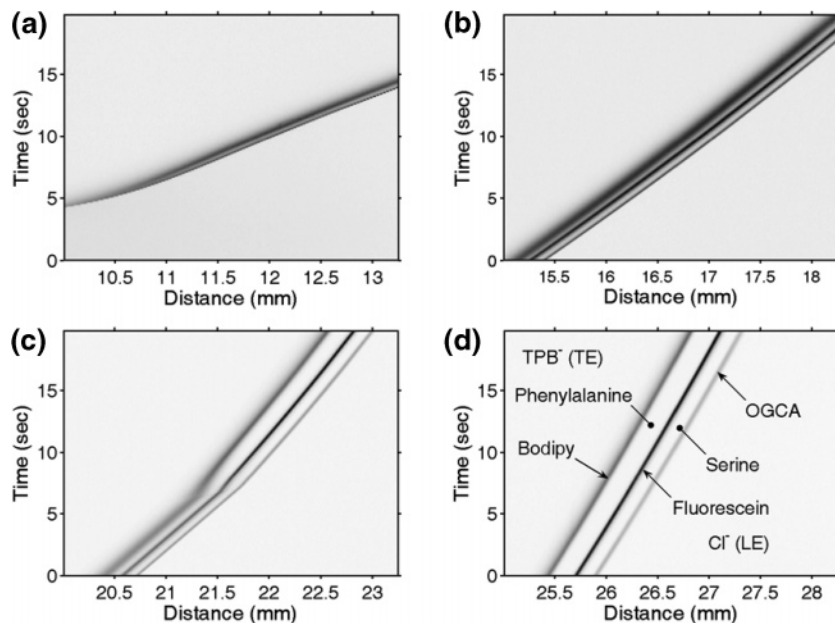


Figure 2. Measurements of marker fluorescence intensity versus time and distance along the 50- μm -wide (by 20- μm -deep) separation channel. Intensity scale is inverted so a dark streak denotes high intensity. The marker bands are initially detectable as a faint, single peak at $x \lesssim 10.5$ mm. The markers then concentrate and separate in a series of phases into three marker peaks. At $x \gtrsim 21.5$ mm, the peaks reach a steady-state velocity (constant slope) and spacing. The three diagonal stripes then clearly describe the location and constant velocity of the three marker peaks. The presence of two unlabeled analytes (phenylalanine and serine) is signaled by two “gaps” between marker bands.

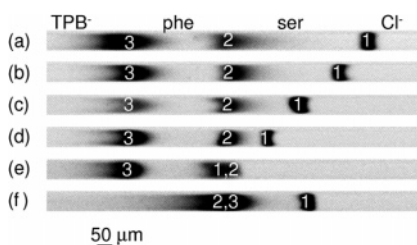


Figure 3. Raw inverted-intensity images of fluorescent marker peaks in a 50- μm -wide (by 20- μm -deep) microchannel, 25 mm downstream of the TE well. Shown are six high LE (350 mM Tris-HCl, pH 10.2) ITP-marker experiments. In cases a–d, the initial concentration of Ser was reduced linearly from 20 to 5 mM, resulting in linear decrease in gap between markers 1 and 2. Phe initial concentration was 10 mM. In (e), only 10 mM Phe was present and markers 1 and 2 became adjacent; and in (f) only 10 mM Ser was present and markers 2 and 3 adjoined. The injected plug length was 6 mm in all cases. Cl^- is chloride; TPB^- is tetraphenylborate; and markers 1, 2, and 3 are respectively OGCA, fluorescein, and Bodipy.

control experiments. A few visualization experiments are shown in Figure 3, and more extensive data are summarized in Figure 4. Figure 3 shows two-dimensional CCD images of the fluorescent markers after achieving steady-state ITP conditions. In (a)–(d), the initial concentration of serine was reduced from 20 to 5 mM, in 5 mM increments; while phenylalanine concentration was fixed at 10 mM. Images e and f in Figure 3 show cases where the analyte solution contained only 10 mM phenylalanine and only 10 mM serine, respectively. The gaps in fluorescent signal (again, dark regions here indicate high fluorescence intensity) caused by serine (Ser) and phenylalanine (Phe) are clearly visible in Figure 3a–d. We observe qualitatively the linear relationship between initial analyte concentration and resulting fluorescent marker gap width. Further, elimination of serine causes the OGCA and fluorescein peaks to become adjacent; while Bodipy and fluorescein peaks adjoin on eliminating phenylalanine. As will be

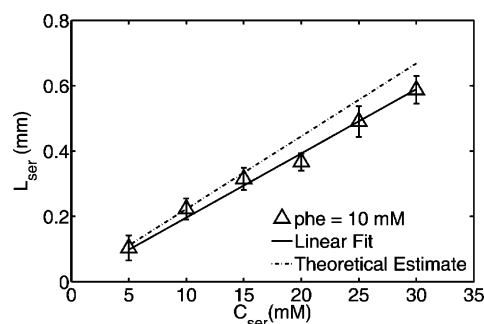


Figure 4. Length of the serine zone at steady state as a function of its initial concentrations for the high LE concentration experiments. Solid line is a linear fit to the experimental data, and the dashed line is the predicted value. Phenylalanine concentration was held constant at 10 mM in these experiments. LE was 350 mM Tris-HCl (pH 10.2), and TE was 50 mM sodium tetraphenylborate.

described below (cf. Figure 8), we can unambiguously identify marker peaks in a single experiment by encoding the identity of these fluorescent markers based on their initial concentrations.

The linear dependence of analyte zone length on initial analyte concentration is shown quantitatively in Figure 4. We performed five realizations for each experimental condition, and error bars were determined from the t -distribution for 95% confidence. The data and its linear fit (shown as a solid line) very closely extrapolate to L_{ser} , indicating that the proportional approximation of eq 3 holds well for this definition of gap width. The gap between adjacent marker peaks is clearly a linear quantification of initial concentration of analyte between those markers. Together with the data of Figure 4, we also plot the theoretical estimate of length ratio predicted by eq 3. The analyte mobilities were estimated using the aforementioned Simul 5.0 software to account for dependence on pH and ion density. The good agreement between predictions and measurements demonstrates the robustness, repeatability, and quantitative nature of the current assay.

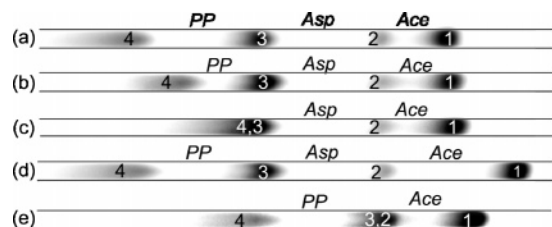


Figure 5. Raw inverted-intensity images of fluorescent marker peaks in a 34- μm -wide (by 12- μm -deep) microchannel, 25 mm downstream from the TE well. Five low LE/high sensitivity ITP-marker experiments are shown. In (a)–(c), the concentration of Ace and Asp was fixed at 20 and 35 μM respectively, and PP concentration was 35, 20, and 0 μM . In (d), the concentration of acetic acid was increased to 45 μM , resulting in an increased gap width between markers 1 and 2. In (e), aspartic acid was eliminated from the analyte mixture and markers 2 and 3 adjoined. The effective length of injected plug was 38 mm, and pressure-driven counterflow was applied from left to right to counter EOF. Here, markers 1, 2, 3, and 4 are respectively OGCA, fluorescein, FITC, and Bodipy.

Low Analyte Concentration Experiments (Low LE Concentration Cases). We performed a set of ITP-marker experiments to explore the sensitivity of this assay for separating and detecting more challenging/lower concentrations of unlabeled analytes. From eq 5, we deduce that high SNR_{an} can be achieved for low initial sample concentration, C_{0,X_i} by increasing injection length, L_0 , and reducing LE concentration, C_L . In these experiments, we therefore reduced LE concentration to 5 mM and increased the length of injected analyte plug to 38 mm to enable detection of ~ 10 μM initial analyte concentrations. As described earlier, we here used pressure-driven flow from cathode to anode to counter EOF. The analytes and markers therefore initially focused into their respective zones 15 mm downstream of the TE well. These zones subsequently migrated at ~ 50 $\mu\text{m}/\text{s}$ toward the anode at steady state.

First, we describe a high-sensitivity experiment in so-called “safe” pH conditions (pH between about 4 and 10, where hydroxyl and hydronium ion concentrations are relatively low compared to other current controlling ions⁴⁶). We present results for the detection and separation of acetic acid (Ace), aspartic acid (Asp) and 3-phenylpropionic acid (PP). We here used four fluorescent markers: OGCA, fluorescein isothiocyanate (FITC) with 200 nM initial concentration, and fluorescein and Bodipy with 50 nM initial concentration. The LE consisted of 5 mM Tris-HCl (pH 9.2), and the TE was 5 mM sodium tetraphenylborate (TPB). Figure 5 shows two-dimensional CCD images of fluorescent markers at steady-state condition. In Figure 5a–c, the initial concentration of Ace and Asp was fixed at 20 and 35 μM , respectively, and the concentration of PP was reduced from 35 μM in (a) to 20 μM in (b) and 0 μM in (c). The gap between markers FITC and Bodipy is accordingly reduced (ultimately to zero) for Figure 5a–c. In (d), Ace concentration was increased to 45 μM , causing the gap width between OGCA and fluorescein to increase correspondingly. In (e), the elimination of Asp from the initial analyte mixture causes the fluorescein and FITC peaks to adjoin. These images qualitatively confirm the linear relationship between the analyte zone length and its initial concentration, as described in eq 3.

(46) Urbánek, M.; Krivánková, L. L.; Bocek, P. *Electrophoresis* **2003**, *24*, 466–485.

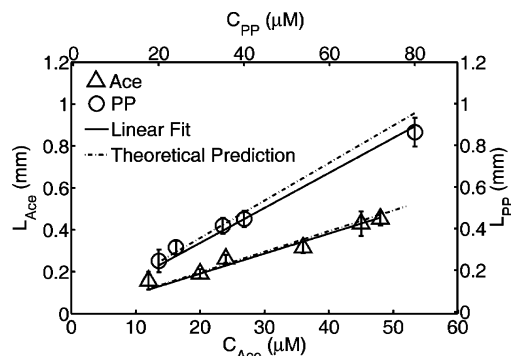


Figure 6. Length of the acetate and phenylpropionate analyte zones as a function of their initial concentrations for the low LE concentration experiment. Solid line is a linear fit to the experimental data with regression coefficient of 0.98, and the dashed line is the theoretical prediction of L_{Ace} and L_{PP} . LE was 5 mM Tris-HCl, and TE was 5 mM sodium tetraphenylborate.

These also serve as validation protocol for our assay since these confirm that the gap between markers is due to the presence of unlabeled analyte.

In Figure 6, the length of acetic acid and phenylpropionic acid zones is plotted against their initial concentration ratio. Here, we varied the initial concentration of Ace from 12 to 48 μM and varied PP initial concentrations from 20 to 80 μM . We quantitatively verify that the length of the unlabeled analyte zone is a linear measure of its initial concentration. Each data point represents three or four realizations per condition (error bars denote 95% confidence). The solid line is a linear fit to the experimental data with a regression coefficient of 0.98. The data are in good agreement with the theoretical prediction of the acetate and phenylpropionate zone lengths obtained from eq 3. We easily achieve a detection limit of 12 μM with excellent repeatability.

Next, as a third example, we discuss the application of our assay to separating and detecting two amino acids, glycine and phenylalanine, with order 20 μM initial concentrations. We used 5 mM Tris-HCl (titrated to pH 10.2 with NaOH) as the LE to ensure a high degree of dissociation of amino acids. The analyte mixture consisted of glycine (20–50 μM) and phenylalanine (20 μM). (We note that we here used serine versus glycine as the mobility of serine was lower than fluorescein at ionic strengths of ~ 5 mM.) We achieved separation of glycine and phenylalanine into two distinct zones bound by the three fluorescent markers. The raw image data for these experiments (similar to Figure 3 and Figure 5) are provided in the Supporting Information (Figure S-2). The 20 μM glycine and phenylalanine were easily detectable in these experiments. The data are qualitatively similar to the other cases, except we observed an increase of the gap length between markers in time, which hinders straightforward quantification of initial analyte concentration. We attribute this effect to the challenges of working outside of the safe pH range. This introduces a fast, high-concentration anion (hydroxyl) into the sample electrolyte and the TE, violating the requirements of anionic ITP. From these and a series of similar experiments, we conclude that the current assay can be readily applied as a detection technique to a wide range of assays; but straightforward quantification of the absolute value of the analyte anion (cation) concentration requires hydroxyl (hydronium) ion con-

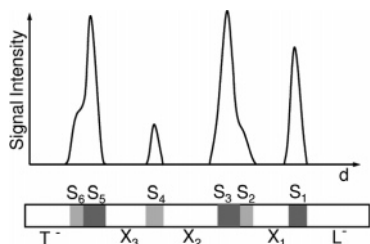


Figure 7. Schematic of repeating high–low concentration encoding scheme applicable to a large number of markers. In spike mode ITP, marker peak intensity is a linear function of its initial concentration. This example assay shows six identifiable markers, S_i , and three analytes, X_i . The relative position of analytes with respect to markers is unambiguously determined by this repeating “high–low” encoding scheme. Encoding can also be accomplished by varying marker color (e.g., alternating between two fluorescence emission wavelengths).

centration to be at least 100-fold lower than the LE concentration (i.e., safe pH).

In comparison, the lowest analyte concentration detected previously using traditional on-chip indirect fluorescence detection methods was ~ 0.4 mM²² (these methods typically detect much higher initial concentrations such as the ~ 0.8 mM detection by Arundell et al.²³). We easily achieve detection sensitivity of ~ 12 μ M with $\text{SNR}_{\text{on}} \sim 4$ with the current technique. Perhaps just as importantly, our assay is free of false peaks, provides a linear measure of initial analyte concentration, and unambiguously bounds analyte mobility to within the resolution of a custom fluorescent marker ladder. We can currently detect as low as 100 nM analyte concentrations using additional preconcentration steps, and we will report this in a future paper.

Concentration Encoding. For a mobility marker ladder consisting of $N + 1$ markers, less than N analytes will result in the merging of two marker peaks, possibly resulting in ambiguity. To eliminate this ambiguity, we propose several simple marker encoding schemes. Encoding can be accomplished spectrally, for example, by using markers with alternating emission fluorescent wavelengths or encoding fluorescence signal intensity by varying the steady-state marker concentration. We here discuss the encoding scheme for the markers based on their fluorescence intensity.

The initial concentration of markers used here has been ~ 50 nM, and so the focused markers in our experiment are in the spike mode where species zone width is determined by the competing effects of dispersion and electromigration. In this regime, the final concentration of markers is a function of their initial concentration (e.g., a regime not captured by eq 1).²⁹ The (spike mode) marker intensity can be “tuned” by changing its initial concentration. Figure 7 schematically shows one such concentration encoding scheme where the concentration of alternating fluorescent markers has been tuned to high- and low-concentration levels. Our arbitrary example shows an assay with three analytes and six fluorescent markers. In the absence of an analyte between the markers, the peaks are adjacent and easily distinguishable. The alternating fluorescence intensity sequence provides unambiguous identification of all marker and analyte zones.

Last, Figure 8 shows a demonstration of this fluorescent marker intensity tuning using the low LE concentration assay (5 mM Tris-HCl, pH 9.2) with four markers and three analytes as described earlier. The initial concentration of acetic acid was 20

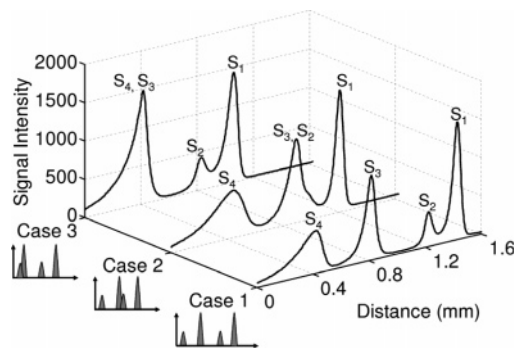


Figure 8. Measurements of fluorescent marker signal intensity versus distance along the separation channel for three ITP-marker experiments (LE: 5 mM Tris-HCl pH 9.2), demonstrating fluorescent marker encoding. Markers S_1 , S_2 , S_3 , and S_4 are respectively OGCA, fluorescein, FITC, and Bodipy encoded with “low” (50 nM) or “high” (200 nM) initial concentration. Cases 1, 2, and 3 are three experimental demonstrations using “high–low–high–low” encodings for markers S_1 , S_2 , S_3 , and S_4 . In case 1, all three analytes, acetic acid, aspartic acid, and phenylpropionic acid, were present, resulting in gaps among the four markers. In cases 2 and 3, aspartic acid and phenylpropionic acid were missing from the analyte solution, respectively, and the corresponding marker peaks adjoined accordingly.

μ M and aspartic acid and phenylpropionic acid concentration was 35 μ M. The initial concentrations of OGCA and FITC were 200 nM and those of fluorescein and Bodipy were 50 nM. This allowed us to achieve a “high–low–high–low” concentration encoding scheme. Three experiments are shown for this encoding scheme. Additionally, aspartic acid and phenylpropionic acid were missing in cases 2 and 3, causing the marker peaks to become adjacent. The markers S_1 , S_2 , S_3 , and S_4 are OGCA, fluorescein, FITC, and Bodipy, respectively. In each case, the low-concentration marker is identifiable even when directly adjacent to a high-concentration marker. Identification and location of each marker is possible regardless of the concentration of the analytes.

Application. The current indirect detection and concentration quantitation assay has several potential applications, including the detection of metabolites in the human body, such as nucleosides, nucleotides, carboxylic acids, purines, and pyrimidines. One interesting application may be the quantitation of the concentration of metabolites in urine samples such as 5-hydroxyindoleacetic acid, homovanillic acid, 4-dihydroxyphenylalanine, ascorbic acid, and uric acid. Abnormal concentration of these are indicators of disease states.^{47,48} Another field of application may be the detection of chemical toxins and wastes such as phenols and alkylcarboxylic acids in water samples.⁴⁹ The U.S. Environment Protection Agency (EPA) restricts the maximum concentration of phenols in drinking water to 1–10 μ g/L, which is difficult to detect with conventional CE with UV detection.⁵⁰

CONCLUSION

We have demonstrated the indirect detection of unlabeled analytes with a technique combining isotachopheresis with

(47) DeQuattro, V. V.; Chan, S. S. *Lancet* **1972**, *1*, 806–809.

(48) Hatch, L. L.; Sevanian, A. *Anal. Biochem.* **1984**, *138*, 324–328.

(49) Sovocool, G. W.; Brumley, W. C.; Donnelly, J. R. *Electrophoresis* **1999**, *20*, 3297–3310.

(50) Rodriguez, I.; Turnes, M. I.; Bollain, M. H.; Mejuto, M. C.; Cela, R. J. *Chromatogr., A* **1997**, *778*, 279–288.

fluorescent markers. The assay displays excellent repeatability and is fairly robust to variations in voltage, pressure head, or electroosmotic flow. Inherent preconcentration of analytes, absence of false peaks, and strong compensation for advective dispersion make the technique attractive over other indirect detection schemes. The length between marker peaks bounding an analyte zone is a linear detector of the analyte concentration. The detection is unambiguous and easy to interpret in the safe pH range (pH between 4 and 10), where the hydroxyl/hydronium ion concentrations are negligible compared to LE concentration. We easily achieve detection sensitivity of 12 μM concentration with SNR_{an} of 4. The analyte resolution is limited only by the resolution of the fluorescent marker ladder used for segregation.

We are now working toward improving the detection sensitivity of our ITP-marker assay and can currently separate and detect ~ 100 nM concentration, which we will demonstrate in a future paper. In its current form, the assay offers a high degree of specificity for a small number of target analytes and markers. We are also working toward the selection and development of "libraries" of fluorescent markers that would greatly improve the dynamic range and the resolution of our assay. We are exploring fluorescent-tagged short DNA fragments and polypeptides as potential marker species.

Last, we note that the concepts of the current assay can be applied to other detection modalities. For example, identifiable markers with strong UV absorption can be used to indirectly detect and quantify the initial concentration of weakly UV absorbing analytes. For electrochemical detection methods (e.g., amperometric detection), strongly electrochemically active markers can be used to detect the presence of analytes with weak electrochemical signals.

SUPPORTING INFORMATION AVAILABLE

Color spatiotemporal plot of the fluorescent markers, raw images of markers in high-sensitivity unlabeled amino acid detection experiments, raw images of markers showing linear dependence of analyte concentration on spacing between markers for high-sensitivity experiments, movie clip of the markers and analyte zones migrating inside the microchannel and spatiotemporal plot for high sensitivity experiments. This material is available free of charge via the Internet at <http://pubs.acs.org>.

Received for review August 12, 2007. Accepted September 25, 2007.

AC701706H